https://doi.org/10.5194/os-2020-115
Preprint. Discussion started: 23 December 2020

Ocean Science
Discussions
Open Access
EGU

Diurnal cycle of the CO_2 system in the coastal region of the Baltic Sea

Martti Honkanen[1], Jens Daniel Müller[2,4], Jukka Seppälä[3], Gregor Rehder[4], Sami Kielosto[1,3], Pasi Ylöstalo[3], Timo Mäkelä[5], Juha Hatakka[5], and Lauri Laakso[1,6]

[1]Meteorological and Marine Research Programme, Finnish Meteorological Institute, Finland
[2]Environmental Physics, Institute of Biogeochemistry and Pollutant Dynamics, ETH Zurich, Zurich, Switzerland
[3]Marine Ecology Research Laboratory, Finnish Environment Institute, Finland
[4]Department of Marine Chemistry, Leibniz Institute for Baltic Sea Research, Warnemunde, Germany
[5]Climate Research Programme, Finnish Meteorological Institute, Finland
[6]School of Physical and Chemical Sciences, North-West University, Potchefstroom Campus, South Africa

Correspondence: Martti Honkanen (martti.honkanen@fmi.fi)

Abstract. The direction and magnitude of carbon dioxide exchange between the atmosphere and the sea is regulated by their difference in partial pressure of carbon dioxide (pCO_2). Typically, observations of pCO_2 are carried out by using research vessels and voluntary observing ships which cannot easily detect the diurnal cycle of pCO_2 at a given location. This study evaluates the magnitude and driving processes of the diurnal cycle of pCO_2 in a coastal region of the Baltic Sea during the different seasons. We present pCO_2 data from July 2018 – June 2019 carried out in the vicinity of the island of Utö in the Archipelago Sea and quantify the relevant physical, biological and chemical processes affecting pCO_2. The highest monthly median diurnal pCO_2 peak-to-peak amplitude (31 µatm) was observed in August. This high diurnal variation was found to be related predominantly to biological processes. The biological transformations of carbon generated a sinusoidal diurnal pCO_2 variation, with a maximum in the morning and a minimum in the afternoon. Compared to the biological carbon transformations, the effect of air-sea excange of carbon dioxide and the effect of temperature changes on pCO_2 are smaller, with their monthly median peak-to-peak amplitudes were up to 12 and 5 µatm, respectively. Single diurnal peak-to-peak amplitudes can be significantly larger (up to 500 µatm), during upwelling. If the net exchange of carbon dioxide between the sea and atmosphere on our study site and sampling period is calculated based on a data set that consists of only one measurement per day, the error in the budget depends on the sampling time and can be up to ±12%.

1 Introduction

During 2008–2017, 10.9 gigatonnes of anthropogenic carbon was released annually into the atmosphere in the form of carbon dioxide (CO_2) mainly through fossil fuel and land use and cement production; approximately a half of these emissions was bound by the terrestrial biosphere, 3.2 $GtCy^{-1}$, and the oceans, 2.4 $GtCy^{-1}$, together (Le Quéré et al., 2018). The increased

https://doi.org/10.5194/os-2020-115
Preprint. Discussion started: 23 December 2020


Ocean Science
Discussions
Open Access
EGU

CO_2 concentration in the atmosphere changes climate globally and the increased CO_2 dissolved in to the oceans generates the ocean acidification (Feely et al., 2009).

The partial pressure of surface seawater CO_2 (pCO_2) and the direction of the air-sea CO_2 flux (F_{as}) are regulated mainly by seasonal biological productivity and respiration, temperature-dependent carbonate chemistry and mixing processes. As the sea surface receives more solar radiation during the day than in the night, a diurnal signal in the biology, physics and chemistry of the surface seawater evolves. Since sea surface pCO_2 information is widely used for calculating the CO_2 exchange between the sea and the atmosphere, there can be large discrepancies between the flux estimates when using pCO_2 values measured at different times of the day.

The diurnal variation of the pCO_2 is typically larger in coastal seas than in the open oceans (Goyet and Peltzer, 1997) due to the larger biological activity. The diurnal pCO_2 cycle has been studied in the oligotrophic ocean (Olsen et al., 2004), coral reefs (Yan et al., 2016) and tidal regions (Andersson and Mackenzie, 2012), while highly productive coastal systems, like the Baltic Sea, have been less researched, even though the Baltic Sea is biogeochemically very complex. Lansø et al. (2017) found that there was no evident diurnal pCO_2 signal in the Baltic Proper and Arkona basin in winter time but during April–October, the monthly average amplitudes were up to 27 $\mu\mathrm{atm}$. Wesslander et al. (2011) determined that in the Baltic Proper, the diurnal pCO_2 variability was controlled either by biological processes, mixing or air-sea exchange of CO_2 at a time. Huge (up to 1604 $\mu\mathrm{atm}$) single diurnal peak-to-peak signals of pCO_2 in a macrophyte meadow in the Western Baltic Sea were reported by Saderne et al. (2013).

The carbon system of the Baltic Sea shows large spatial variability. On the one hand, the Northern parts of the Baltic Sea, i.e. the Gulf of Bothnia, are characterized by large fluvial fluxes of organic matter into the basins, which through effective bacterial mineralization turns the area to a source of CO_2 to the atmosphere (Algesten et al., 2006). On the other hand, the southern parts of the Baltic Sea exhibit larger primary production compared to the Gulf of Bothnia (Wasmund et al., 2001), larger input of alkalinity and lower organic matter input, which makes the basin act as a sink (Kuliński and Pempkowiak, 2011). Based on a mass balance approach of Kuliński and Pempkowiak (2011) and revisited by Ylöstalo et al. (2016), the Baltic Sea as a whole is considered to be a weak source of carbon dioxide to the atmosphere.

Measurements of pCO_2 hosted on voluntary Observing Ships (VOS) have proved to be a cost-effective method to reveal new insights of spatio-temporal variability of the Baltic Sea's carbon cycle (Schneider et al., 2014; Schneider and Müller, 2018). These surface pCO_2 measurements carried out on VOS-routes are currently our best presentation of the spatial variability of CO_2 partial pressure in the Baltic Sea. However, these measurements carried out on fixed routes and time schedules do not resolve the diurnal cycle and when interpreting these data, one should consider the potential bias caused by the time of the sampling. Fixed platforms capable of measuring in high temporal resolution can resolve the diurnal cycle of carbon.

In this contribution, we investigate the diurnal cycle of carbon dioxide system at the fixed station. Utö, located in the transition zone between Northern Baltic Proper and Archipelago Sea represents highly productive coastal ecosystem. The aims of this study are (a) to investigate the diurnal cycle of pCO_2 during different seasons based on observations carried out at Utö and (b) to quantify the magnitude of main phenomena affecting the pCO_2 diurnal variations: air-sea flux, biological carbon uptake and release and diurnal changes in temperature.

https://doi.org/10.5194/os-2020-115
Preprint. Discussion started: 23 December 2020


Ocean Science
Discussions
Open Access
EGU

2 Controls on the partial pressure of CO_2

The surface pCO_2 can be altered by processes that alter dissolved inorganic carbon (DIC) or total alkalinity (TA) or affect the chemistry of the carbonate system through changes in temperature, salinity or pressure (Takahashi et al., 1993).

2.1 Carbon control of pCO_2

As dissolved inorganic carbon (see Appendix B) is introduced to or removed from the dissolved inorganic pool, the change of dissolved CO_2 concentration is depicted by the so-called Revelle factor, Re (Sarmiento and Gruber, 2004):

$$Re = \frac{\Delta[\mathrm{CO_2}]}{[\mathrm{CO_2}]} / \frac{\Delta DIC}{DIC} \tag{1}$$

DIC in surface water can be altered by the CO_2 exchange with the atmosphere, biological transformations, precipitation/dissolution of calcium carbonate, fresh water input and mixing of water masses. The freshwater input includes evaporation, precipitation and the formation and melting of sea ice. Fresh water effect is likely negligible in diurnal time scale for the mixed layer deep enough. Biological processes affecting pCO_2 include all transformations between the inorganic and organic carbon pools, i.e. photosynthesis and respiration. The mixing processes include horizontal advection, vertical diffusion and vertical entrainment. Arguably, mixing processes are random in nature and do not show diurnal cyclicity and thus do not affect our analysis.

2.2 Alkalinity control of pCO_2

TA (see Appendix C) is altered mainly by the formation and dissolution of calcium carbonate. Smaller contribution to TA originates from nitrogen transformations through biological processes, fresh water balance and the mixing processes. TA is not affected by the air-sea exchange of CO_2. The effect of calcifying primary producers on the carbon pool in the Baltic Sea can be neglected for open sea (Tyrrell et al., 2008). However, calcifyers may have an effect on carbon cycle in benthic zone.

2.3 Physical control of pCO_2

Temperature affects the dissociation constants and solubility, which further alters the CO_2 partial pressure. For the stable oceanic conditions, this change is well documented (Takahashi et al., 1993), but in estuary conditions, the value varies significantly (Schneider and Müller, 2018). Based on the choice of the parametrization of dissociation constants, this value might show small variation as a function of temperature and salinity (Orr et al., 2015).

Similarly to temperature, also salinity affects the dissociation constants. However, salinity changes are related to mixing, and thus the interpretation of salinity effect is not straight-forward and is not dealt with in this paper. The salinity effect on pCO_2 is generally small: in oceanic conditions, a salinity change of 1 would generate a 9 $\mu\mathrm{atm}$ change in pCO_2 (Sarmiento and Gruber, 2004). At Utö, the salinity varies less than 1.5 PSU during the whole year (see Fig. 1).

We neglect the effect of pressure on pCO_2, because we are dealing with surface water pCO_2 at one depth.

https://doi.org/10.5194/os-2020-115
Preprint. Discussion started: 23 December 2020

2.4 Included processes controlling pCO_2

In this study, we are considering the pCO_2 changes that are generated by the changes in DIC or by temperature fluctuations. DIC changes are further divided into the changes that are caused by the air-sea exchange of CO_2 or by the biological transformations. There are multiple processes affecting the pCO_2 that are not included in the analysis.

Some of these unknown drivers, such as mixing processes and fresh water effects, are assumed to be temporally random in nature and thus their effect on pCO_2 is considered to be negligible when inspecting average cycles. Some of the processes, e.g. alkalinity related variations affecting pCO_2 are unknown and may involve diurnal cyclicity. A salinity-alkalinity relationship used in the analysis takes into account the conservative variation of these variables due to the mixing and freshwater input. Nitrogen transformations during primary production can have small effect on alkalinity that is not considered in the salinity-alkalinity relationship.

In the results, we analyze applicability of the method by comparing the calculated pCO_2 changes to the observed changes.

3 Materials and methods

The Utö Atmospheric and Marine Research Station is located on the small island of Utö in the southern edge of the Archipelago Sea (59°46'55" N, 21°21'27" E). The marine observations ("marine station") at the station focus on regional marine ecosystem functioning with a large number of biochemical and physical observations. The atmospheric part of the station include a wide range of meteorological, trace and greenhouse gas and aerosol measurements. Greenhouse gas and some meteorological measurements are part of ICOS (Integrated Carbon Observation System) atmospheric station network. Marine measurements of Utö Atmospheric and Marine Research Station belong to Joint European Research Infrastructure for Coastal Observatories (JERICO-RI, www.jerico-ri.eu). Carbonate system dynamics is noted as one of the key scientific topics in the coastal ocean (Farcy et al., 2019) and the current study, done under framework of JERICO-RI, highlights the need for integrated and multidisciplinary observations. For detailed list of observations, site bathymetry and other information about the station, please see Laakso et al. (2018).

Our study is based on one year of data gathered between July 2018 and 2019. All data presented in this paper is given in the UTC time. Finland belongs to the UTC+2:00 timezone.

3.1 Flow-through sampling

The marine station is equipped with a flow-through pumping system that transports water from 250 m from the shore to the station, where seawater is analyzed automatically and manually on demand. The bottom-moored floating seawater inlet is approximately at the depth of 4.5 m $\pm$ 0.5 m. The mean depth at this location is 23 m and the sea level at Utö varies $\pm$ 0.5 m relative to theoretical mean sea level.

At the station, the transported water first enters a manifold. Any flow-through instrument can be attached to the manifold separately, enabling arbitrary adjustment of the flowrate for each instrument.

https://doi.org/10.5194/os-2020-115
Preprint. Discussion started: 23 December 2020


Ocean Science
Discussions
Open Access
EGU

All of the instruments attached to the flow-through system are automatically washed with cleaning fluid (Hydrogen peroxide or Triton X-100) daily. The data gathered during and immediately after the cleaning have been discarded.

Most of the instruments that analyze seawater logged data every 15 s. These data are shifted ($5.6\,\mathrm{min}$ on average) according to the concurrent flow rate (54–68 LPM) to match the time of sampling at the intake, based on the known volume of the pipe system.

3.2 Measurement of pCO_2 and CO_2

pCO_2 was measured using a SuperCO$_2$ instrument (Sunburst Sensors), which was connected to the flow-through system. In its two shower-head equilibrator chambers, the seawater CO$_2$ is equilibrated with the gas above according to Henry's law (Eq. B2). The equilibrated gas leaves the chamber for an infrared gas analyzer (LI-840A, LI-COR), where CO$_2$ molar fraction (xCO_2) is measured. The sensor drift of the gas analyzer is taken into account by measuring every fourth hour four standard gases with differing CO$_2$ molar fractions (0.00, 234.38, 396.69 and 993.45 ppm, $\pm 2\%$) in order to form a correction equation for dry xCO_2. These standard gases are produced and verified by Finnish Meteorological Institute. Drift-corrected dry xCO_2 is transformed into pCO_2 according to Dickson and Goyet (1994). One hour median values are used in the final analysis of pCO_2 changes.

Since the sample water temperature decrease (in summer) during the transport due the colder bottom water temperatures passed by the water line, we took the effect of temperature change on pCO_2 into account using the CO2SYS matlab program. This correction requires that knowledge of another carbon system component, which is total alkalinity (from salinity) in our case. The equilibrator temperature (together with salinity) was measured using a thermosalinograph (SBE45 MicroTSG, Sea-bird Scientific) next to the SuperCO$_2$ instrument. The in situ temperature was measured using a PT-100 thermometer at the depth of $3\,\mathrm{m}$ at the upper level of the thermistor chain near the inlet. On average, seawater cooled when transported, $0.4 \pm 2.0\,^{\circ}\mathrm{C}$.

In May-June 2019, the sampling and inlet tube system was tested by measuring CO_2 concentrations with two SAMI^2 sensors (Sunburst Sensors) parallel to the SuperCO$_2$ system inside the measurement station (20–23 May 2019), after which the SAMI^2's were deployed next to the sampling inlet in the sea (24 May – 7 June 2019). The parallel measurement inside the station was used to correct the potential initial offset of the SAMI sensors, against the SuperCO$_2$ system. When the SAMI^2 sensors were in the sea, the in-situ concentrations for all three instruments closely followed each other and no impact on pCO_2 observed by SuperCO$_2$ was found: the root mean square difference between the between the sea inlet and the station was $4.1\,\mu\mathrm{atm}$. The difference, or the absolute values, do not influence the analysis of diurnal cycle.

Atmospheric CO$_2$ molar fractions were measured at the Atmospheric ICOS site using cavity ring-down spectroscopy (Kilkki et al., 2015).

3.3 Other flow-through measurements

Oxygen was measured with an oxygen optode (Aanderaa 4330) with multipoint calibration. Chlorophyll A was measured with Wetlabs FLNTU fluorometer, as a proxy of chlorophyll concentration, using factory calibration. Both were connected to the flow-through system. Chlorophyll A measurement was offline in winter (January–March).

https://doi.org/10.5194/os-2020-115
Preprint. Discussion started: 23 December 2020


Ocean Science
Discussions
Open Access
EGU

3.4 Hydrographic measurements and determination of mixed layer depth

The vertical temperature profiles were measured with temperature chains, supported with regular interval CTD (Conductivity-temperature-depth) profiles. In this paper, we use the the measurements of a chain that was deployed 150 m northeast from the seawater inlet in July 2018: this chain was moored at the depth of 21.3 m ± 0.5 m, and its Pt-100 thermistors were placed at the heights of approximately 18 m, 13 m, 8 m, 1 m and 0 m from the bottom (depths 3.3 m ± 0.5 m, 8.3 m ± 0.5 m, 13.3 m ± 0.5 m, 20.3 m ± 0.5 m, 21.3 m ± 0.5 m). The depth closest to the surface was selected based on wave and sea ice cover observations, in order to avoid instrument damages during the rough weather conditions.

The mixed layer depth (z_{mix}) was determined from the temperature vertical profiles which were measured using a CTD (RBR XR-620) approximately 400 m west of the sampling inlet. CTD profiles were taken by local Ismo Willström by using a small boat, fortnightly during the productive period and with lower temporal resolution in winter (see Fig. 1). Eventhough the data by the thermistor chain has higher temporal resolution than the CTD castings it is not applied for the assessment of the mixed layer depth, because it has significantly lower vertical spatial resolution. The water depth at the location of CTD castings is approximately 90 m, which is significantly deeper than the depth at the inlet location. If the mixed layer depth was larger than the depth of 23m at the inlet location, the water column at the inlet location was considered mixed. The thermocline depth, i.e. the depth of the strongest temperature gradient in the profile, was considered to represent z_{mix}. For each CTD cast, a thermocline depth was estimated. Due to the marked horizontal distance between the inlet and CTD profiling, the applicability was assessed by comparing these CTD measurements to the Pt-100 thermistor chain measurements near the inlet, which confirmed relatively good match of the measurements with the root mean square difference of 0.6 °C. The CTD measurements reproduced well the hydrography of the upper water column at the inlet location, as the root mean square differences between the sites for the depths of 3, 8 and 13 m were 0.42, 0.41 and 0.25 °C, respectively. The temperatures at 20,m, however, showed larger difference, as the RMSE was 1.08 °C for this depth. This implies that the mixed layer depths were well reproduced using the CTD castings unless the thermocline was be located close to the bottom of the inlet location.

3.5 Estimation of F_{as}

The estimation of the air-sea exchange of CO_2 between the sea and atmosphere is based on two methods: 1) on the the eddy covariance method from the data gathered using a micro-meteorological flux tower erected on the western shore of the island and 2) on the wind speed based flux parametrisation. Due to strict quality control, the eddy covariance method was applicable for only 18% of time, and for the rest of the time, the parametrisation was used.

Both methods have pros and cons, due to which they complement each other. The eddy covariance method considers the integrated flux within large footprint area, whereas the parametrization is based on the pCO_2 measurement at single point at the depth of 5 m. The large footprint area may contain spatially heterogeneity in seawater pCO_2. In some cases, the measurement at the depth of 5 m may not represent the surface conditions. Additionally, the parametrization of gas transfer velocity is based on the wind speed, which solely does not contain all the information about the surface turbulence.

https://doi.org/10.5194/os-2020-115
Preprint. Discussion started: 23 December 2020


Ocean Science Discussions

3.5.1 Eddy covariance method

The eddy covariance fluxes for air-sea exchange of CO_2 were calculated for 30 min intervals. This flux measurement is based on the closed-path non-dispersive infrared gas analyzer (LI-7000, LI-COR), of which sample air tubing has a 30 cm Nafion drier (PD-100T-12-MKA, Perma Pure) in order to eliminate the water vapor interference on CO_2 fluxes. The covariance of 10 Hz vertical wind velocity (w) and CO_2 molar fraction (xCO_2) data was calculated for each 30 min averaging period. These fluxes were corrected for the high-frequency attenuation by using a transfer function which was calculated from the deviation of the normalized w-CO_2 cospectrum from the one of sensible heat flux. Only stationary CO_2 flux conditions were included, because during non-stationary conditions, the measured fluxes do not represent the exchange between the surface and the atmosphere. Only western winds were considered (180–330 °) here as the flux footprint during these cases originates from the sea. Small amount of flux data were excluded from the analysis because the reference gas pipeline for the CO_2 analyzer was leaking. More information about the flux system and its quality control can be found in Honkanen et al. (2018).

3.5.2 Flux parametrisation

We used an air-sea exchange estimation based on the quadratic relationship by Wanninkhof (2014) for the times without valid eddy flux measurements (82%). Wind speed was measured with the micrometeorological flux tower on the westenr shore, and data were converted to wind speed at the height of 10 m, U_{10}. As the wind speed is not precisely measured at the height of 10 m, we corrected wind speed assuming a logarithmic wind profile and a constant surface roughness of 0.5 mm, a value which is based on the data of Honkanen et al. (2018). More details about the compatibility of the parametrization for this specific site can be found in the Appendix D.

3.6 Calculation of pCO_2 changes generated by different processes

Calculations were performed using the CO2SYS matlab program. Dissociation constants K_1 and K_2 were calculated based on Millero (2010) and the sulfate contribution is based on Dickson (1990). We implemented the total boron parametrisation by Kuliński et al. (2018), which is based on the empirical data of the Baltic Sea, in CO2SYS.

We use total alkalinity as a second carbon system variable in our calculations. The total alkalinity used here is based on alkalinity-salinity relationship, which was determined by using the titration measurements carried out at Utö in summer 2017 (Lehto, 2019):

$$TA(\mu\mathrm{mol\,kg^{-1}}) = 123.3 + 221.8 \cdot S, \tag{2}$$

The slope is almost identical to the dependence found for the Gulf of Bothnia by Müller et al. (2016) extrapolated for year 2017. See Appendix C for more information.

First, the carbon chemistry is calculated for each hour based on the measured partial pressure of CO_2 and parameterised total alkalinity. This way, we know the DIC at every starting step. Hourly mean values are used thorough this analysis.

https://doi.org/10.5194/os-2020-115
Preprint. Discussion started: 23 December 2020


Ocean Science
Discussions
Open Access
EGU

The effect on temperature fluctuations on the diurnal cycle of pCO_2 was calculated in CO2SYS using the TA and previously calculated DIC with the temperature of the next hour. The effect of temperature changes on pCO_2 is then quantified as the difference between this pCO_2, that is affected only by the temperature change, and the original pCO_2.

In the case of air-sea exchange and biological transformations, we calculated how much DIC changed over one hour and add this $\mathrm{d}\,DIC$ to the original content. We assume that total alkalinity does not change in the process, and calculated the carbon system using this new DIC and the total alkalinity in order to get the new pCO_2.

We assume that the new inorganic carbon ($\mathrm{d}\,DIC_A$) derived from the air-sea exchange of carbon dioxide is evenly distributed within the mixed layer. DIC change due to the air-sea exchange of CO_2 is calculated as:

$$\mathrm{d}\,DIC_A = \frac{F_{as}}{z_{mix}}\Delta t, \tag{3}$$

where t is time, i.e. one hour. The value of F_{as} is calculated using either the eddy covariance method or the wind speed based parametrization depending on the concurrent wind direction and the flux stationarity.

We inferred the biological effect on DIC indirectly from the oxygen measurements by assuming the Redfield ratio (Redfield et al., 1963). As inorganic carbon is consumed (or released), a relative amount of oxygen is released (or consumed),

$$\mathrm{d}\,DIC_B = -\frac{106}{138}\Delta[\mathrm{O_2}] - \frac{FO_2\Delta t}{z_{mix}} \tag{4}$$

The ratio of 106 C : - 138 O refers to the Redfield ratio of carbon to oxygen (Redfield et al., 1963). However, this ratio is based on average oceanic conditions and may show variations in space and time. The last term in the equation takes the effect of air-sea exchange of oxygen into account. This flux, FO_2, is calculated similarly to the carbon dioxide flux (Eq. A1) by using the gas transfer velocity, (oxygen) solubility and (oxygen) concentration gradient. Oxygen solubility was calculated according to the salinity-temperature dependence fit by Garcia and Gordon (1992) which is originally based on Benson and Krause (1980). The Schmidt number of oxygen and gas transfer velocity were calculated according to Wanninkhof (2014). Oxygen can also change due to the mixing, whose contribution remains unknown.

We examined the diurnal fluctuations of pCO_2 by examining each day at a time. For each day, the cumulative sums of the pCO_2 changes generated by different processes were calculated, and finally the mean of cumulative sum was removed from these values:

$$pCO'_{2,i} = \sum_{i=1}^{24}\Delta pCO_{2,i} - <\sum_{i=1}^{24}\Delta pCO_{2,i}> \tag{5}$$

where i is the index of each hour and angle brackets denote the averaging.

In addition to the pCO_2 evolution generated by the air-sea exchange of CO_2, biological transformations and temperature alone, we also examined the pCO_2 evolution generated by these three processes simultaneously. This is calculated using the new DIC that is altered by both air-sea exchange of CO_2 and biological transformations and additionally taking into account the temperature change. However, this pCO_2 change is only used for the verification of the method.

https://doi.org/10.5194/os-2020-115
Preprint. Discussion started: 23 December 2020

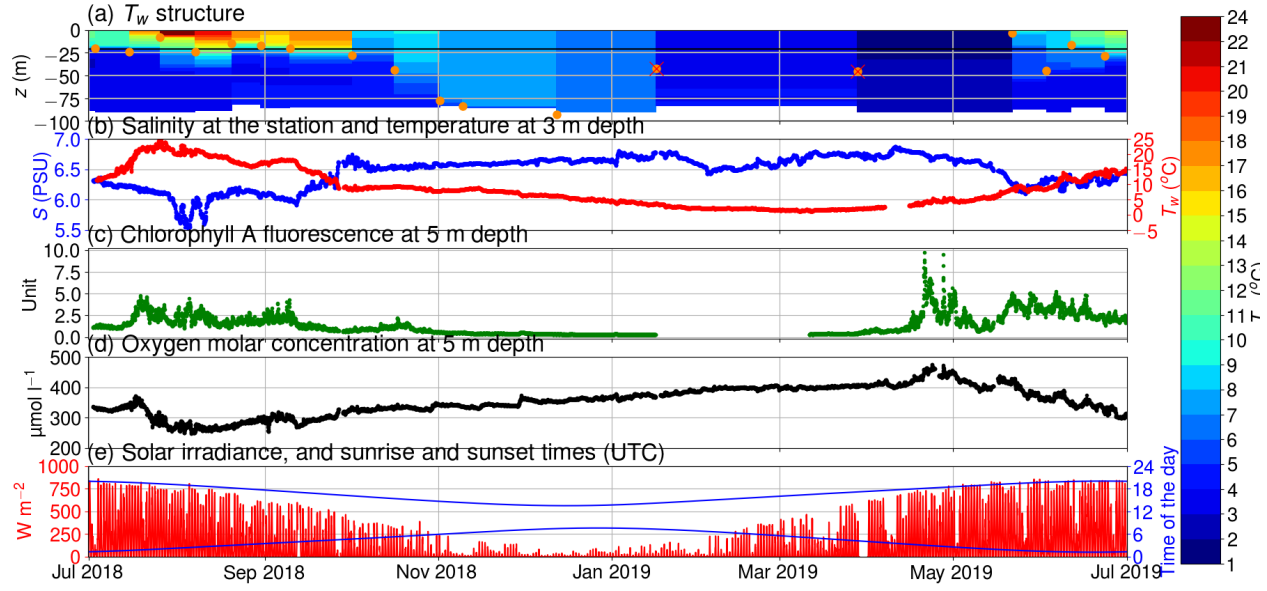

Figure 1. (a) Temperature of the seawater (T_w) and depth of thermocline depth (orange circle), the thermocline depth with questionably small (< 0.2 °Cm^{-1}) temperature gradient has red cross on it, the horizontal solid black line depicts the depth at the inlet location; (b) salinity and temperature at 5 m depth; (c) Chlorophyll A fluorescence as a proxy for concentration at 5 m depth; (d) Oxygen molar concentration at 5 m depth; (e) solar irradiance (red) and sunrise and sunset times (blue) in UTC.

Throughout the results, we use the range, r, to describe the diurnal pCO_2 variability. The range, or the peak-to-peak amplitude, is defined as a difference between the diurnal pCO_2 maximum and minimum:

$$r = \max(pCO_2) - \min(pCO_2) \tag{6}$$

4 Results and discussion

4.1 Environmental conditions

The measuring period started in July 2018, during phytoplankton summer minimum in the Baltic Sea (Andersson et al., 2017). Chlorophyll A concentration was low, reflected as a low relative fluorescence unit (Fig. 1c). In mid-July, the summer cyanobacteria bloom developed, as typical for the study area (Kraft et al., 2020), which lowered the pCO_2 below 200 µatm for ca month (Fig. 2a). Another small bloom occurred in early September. In late September 2018, pCO_2 peaked at 800 µatm, which is likely a result of mixing with the sub-thermocline water masses that have high DIC due to the remineralization of organic matter, which is supported by the deepening of the mixed layer depth (Fig 1a). In winter, the pCO_2 slowly equilibrated with

https://doi.org/10.5194/os-2020-115
Preprint. Discussion started: 23 December 2020

the atmosphere. Chlorophyll A fluorescence peaked again in April 2019 as a result of spring bloom. Simultaneously, the pCO_2 dropped to 200 µatm, where it stayed for two months. The sea was a sink of atmospheric carbon for approximately 4 months a year. Generally, the seasonality of pCO_2 at Utö is similar to the open pelagic conditions in the Baltic Proper (Wesslander et al., 2010) but the maximum value (800 µatm) in autumn is considerably higher than observed in the Baltic Proper (600 µatm). This could be due to the fact that the measurement location is relatively shallow and thus has stronger component from bottom mineralization.

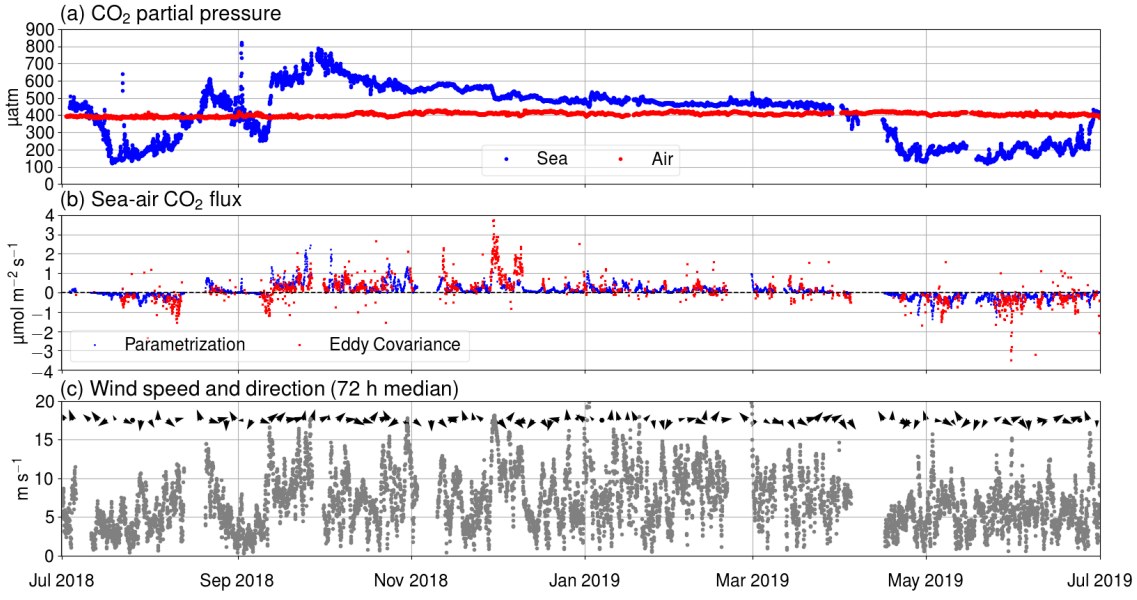

Figure 2. (a) pCO_2 of air (red) and of seawater (blue), (b) FCO_2 measured using Eddy covariance method (red) and calculated using Eq. A3 and (c) wind speed (gray dots) and direction (black arrows).

The thermocline was predominantly at the depth of 20 m during the summer of 2018. In autumn, the thermocline deepened and in mid-winter the water column was considered to be thoroughly mixed. Only in few cases, the thermocline may have been shallower than the inlet depth, e.g. in spring 2019, when the shallow thermocline formed quickly. Therefore, in most of the time our flow-through setup was sampling the water from the mixed layer. This supports the assumption that there were no fresh water lenses or they were so short-lived that they do not play any role on the analysis. There was no permanent ice cover during the measurement period.

4.2 Examples of diurnal pCO_2 variability

Examples of pCO_2 diurnal variability in the beginning of September 2018 are given in Fig. 3.

https://doi.org/10.5194/os-2020-115
Preprint. Discussion started: 23 December 2020

Ocean Science
Discussions
Open Access
EGU

On the 3rd of September 2018, we observed that pCO_2 showed a range (maximum - minimum) of 108 µatm. The oxygen-derived biological pCO_2 diurnal cycle shows closely similar evolution, indicating that this large pCO_2 diurnal variability is a result of biological transformations. However, some deviation between observations and calculations solely based on oxygen dynamics (i.e. diurnal biological transformations) is evident early in the morning and late in the evening. The air-sea exchange had negligible effect on the pCO_2 on that day, because the CO_2 partial pressure difference between the sea and atmosphere was close to zero. It is interesting that the inclusion of temperature into the model does not increase the fit in this case, instead it increases the deviation between the observation and model. It is possible that the oxygen-derived biological component is too small: if the biological component was larger, the temperature component would partly compensate it and thus making a better fit with the observations. In the chapter 4.2.5, we give an evidence of slightly too small biological component in September.

On the 2nd of September 2018, the pCO_2 showed much larger variation (452 µatm), but generally, the sinusoidal shape of the diurnal variation was closely similar to the one on the 3rd day. On both days, pCO_2 had the highest change rate at 9 UTC. The diurnal evolution supports the theory that even this large pCO_2 variation at this location could be generated by biological transformations. Again, we notice that the oxygen-derived biological component gives lower variability than observed.

The Largest (503 µatm) pCO_2 range was detected in 22nd of July, but this rare case was clearly generated by an upwelling event, as the water cooled 8 C simultaneously. This particular case is discarded from the following pCO_2 diurnal analysis.

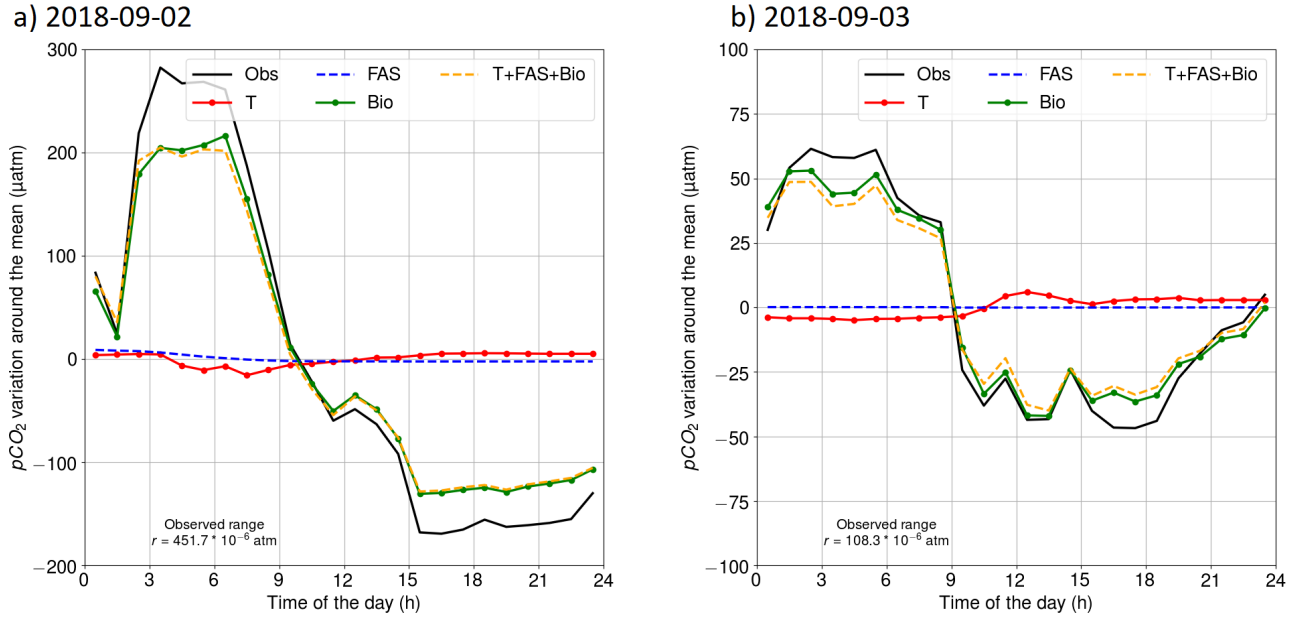

Figure 3. pCO_2 diurnal variability on a) the 2nd of September 2018 and b) the 3rd of September 2018. Black line is the observed (Obs) evolution. Other lines are the calculated pCO_2 evolution generated by different processes: red for temperature (T), blue for air-sea exchange of carbon dioxide (FAS), green for by biological transformations (Bio) and orange for the combined effect of all mentioned processes (T+FAS+Bio).

https://doi.org/10.5194/os-2020-115
Preprint. Discussion started: 23 December 2020

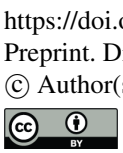

Ocean Science
Discussions
Open Access
EGU

4.2.1 Observed diurnal pCO_2 variability

The observed diurnal variability of pCO_2 was lowest during the winter time (Fig. 4): the monthly median range (maximum - minimum) in November–February was only 4 µatm. In February the monthly median range and the range between the 10th and 90th percentiles are lowest: less than 11 µatm daily variation is expected for 80% of the time. In winter time, no clear diurnal pattern is visible, which is also indicated by the varying times for the daily minimum and maximum pCO_2. The absence of clear diurnal pattern in pCO_2 during winter is consistent with the findings of Lansø et al. (2017) for the Baltic Sea Proper.

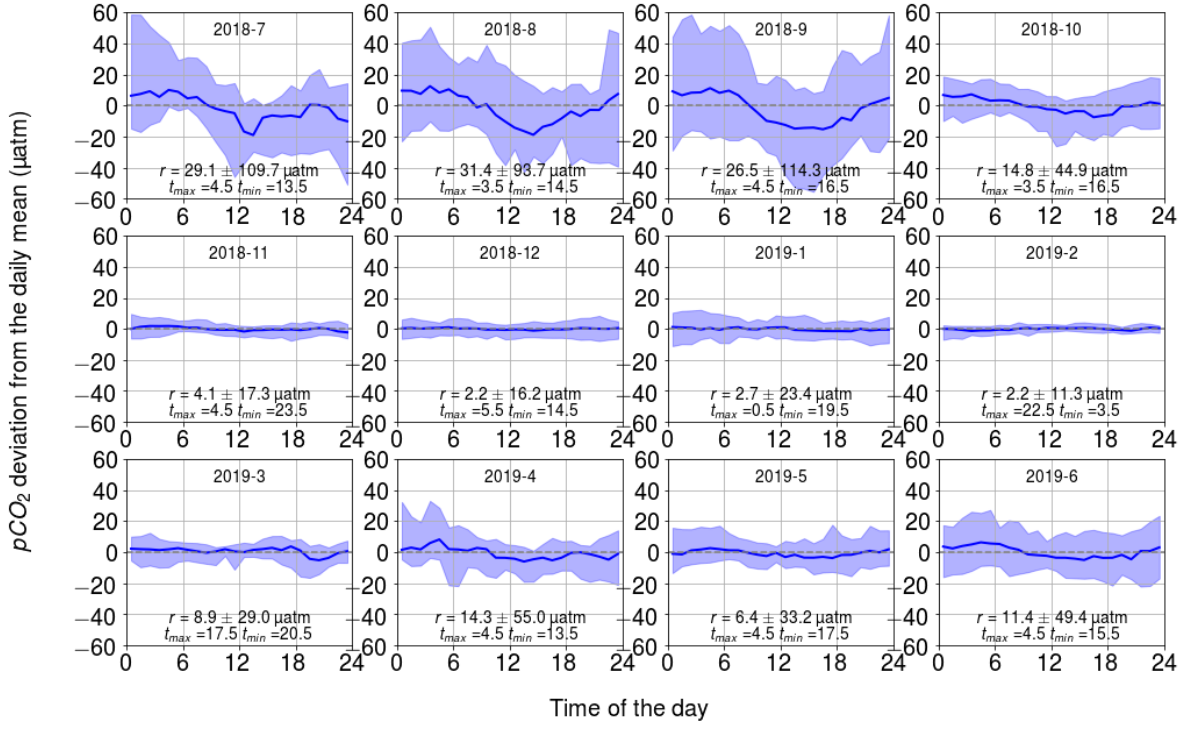

Figure 4. Observed monthly pCO_2 diurnal variability, showing the binned median and difference of minimum of 10th and maximum of 90th percentiles. The y-axis has the pCO_2 deviation in µatm and the x-axis is the hour of the day. Range, r, and the time for the maximum and minimum pCO_2 are also given.

In April, the observed diurnal pCO_2 variability starts to show a sinusoidal form, which remains until October. The diurnal pCO_2 minimum occurs during the afternoon and the maximum in early morning. At approximately 9 o'clock UTC (12 o'clock local summer time), the pCO_2 is closest to the diurnal mean. The monthly median range of pCO_2 increased until August, which had the highest monthly median range of 31 µatm. In the Baltic Proper, the highest diurnal pCO_2 variability (27 µatm) is met one month later, in September (Lansø et al., 2017). The difference between these two datasets might be due to the interannual

https://doi.org/10.5194/os-2020-115
Preprint. Discussion started: 23 December 2020

variability, as different years are compared, or it might indicate the effect of slightly longer growing season for the Baltic Proper, or the benthic production/respiration may have larger role in our shallow station than it has in pelagic Baltic Proper. There is large variability in diurnal pCO_2 over the course of a single month during the productive season: a single day may deviate significantly from the monthly median value as, based on the 10th and 90th percentiles, 80% of the days in September have the range less than 114 µatm.

4.2.2 Temperature-related diurnal pCO_2 variability

The diurnal pCO_2 variability generated by temperature is generally small (Fig. 5). Apart from June, July and August, the monthly median range was 3 µatm or less. The largest monthly median range occured in July (5 µatm), when the solar irradiance has its annual maximum (Fig. 1e). Still, for 20% of the days in July, a temperature-related diurnal variability of $pCO_2 > 27$ µatm was observed.

During months with high solar radiation, March–September (Fig. 1e), the maximum of the temperature-related diurnal pCO_2 cycle occurs at noon and the minimum in the middle of the night or in the early morning. In winter, the temperature-related pCO_2 does not show clear variation. We would expect a decline of the temperature-related pCO_2 in winter time, but the effect is probably small.

The measurement depth of the temperature is 3 m. For the surface conditions we would expect higher temperature-related pCO_2 variability since the solar irradiance penetrating the water column decreases with the depth.

4.2.3 Diurnal pCO_2 variability generated by air-sea CO_2 flux

The pCO_2 diurnal fluctuations generated by air-sea exchange of CO_2 exhibits a clear trend-like pattern (Fig. 6), due to the nature of the process. This exchange drives to balance the CO_2 pools between the sea and atmosphere.

The effect is largest in September-October when the partial pressure difference and the wind induced mixing are largest. In September, the monthly median range was 10 µatm. When the sea and atmosphere were nearly balanced with respect to pCO_2 as in December-March, or when the wind speeds are low as in summer months, the effect of air-sea exchange on diurnal pCO_2 variability is almost negligible (less than 2 µatm).

The mixed layer depth has an effect on this pCO_2 diurnal variability. However, the turbulent mixing that drives the CO_2 exchange between the sea and atmosphere, also deepens the mixed layer.

4.2.4 Biology related diurnal pCO_2 variability

The diurnal pCO_2 signals calculated from the oxygen data are closely similar to the observed ones (Figs. 3, 4 and 7). Sinusoidal diurnal variability with the maximum in the morning and the minimum in the afternoon during April-September is observed in both cases and the monthly median ranges are of same order. During the nighttime respiration (both heterotrophic and autotrophic) prevails and pCO_2 increases. Solar irradiance intensifies as the day progresses and the carbon fixation outweighs

https://doi.org/10.5194/os-2020-115
Preprint. Discussion started: 23 December 2020

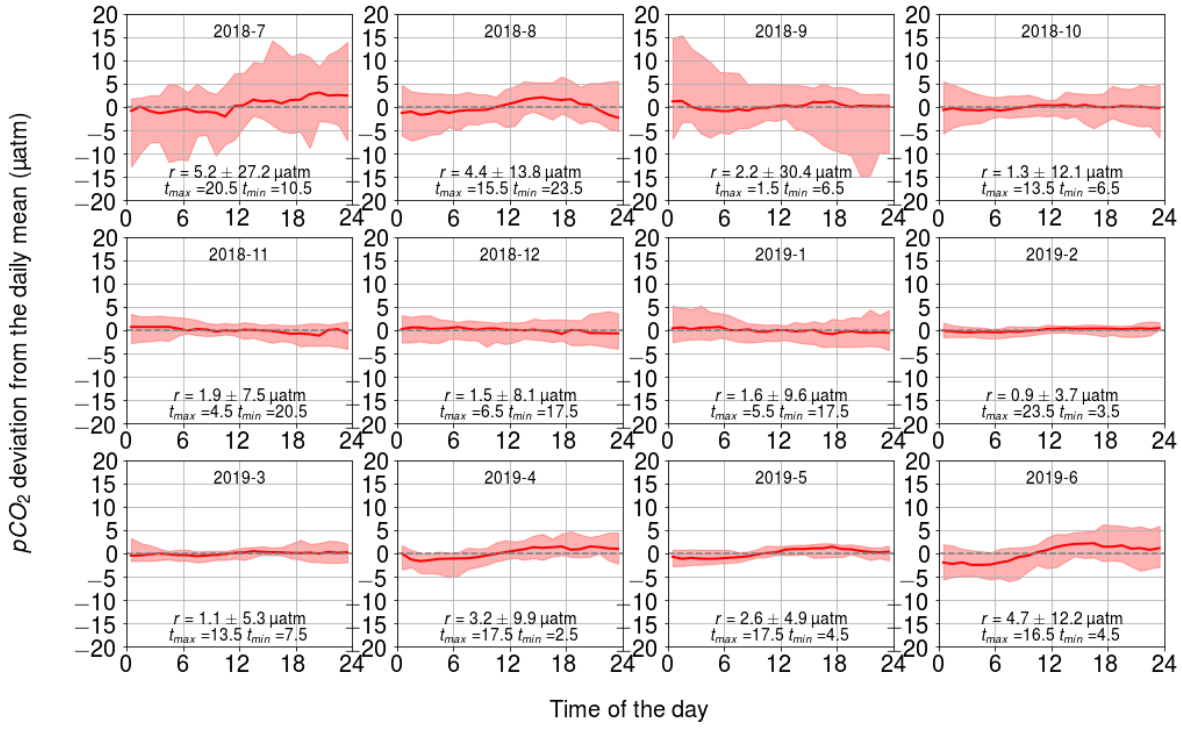

Figure 5. Temperature induced cumulative daily changes in pCO_2, shown as monthly climatological median and difference of minimum of 10th and maximum of 90th percentiles. The y-axis has the pCO_2 deviation in $\mu\mathrm{atm}$ and the x-axis is the hour of the day. Range, r, and the time for the maximum and minimum pCO_2 are also given.

the respiration. For our shallow measurement location, it is possible that the benthic processes may have an effect on the carbon system, especially when the water body is completely mixed.

In summer, the increasing temperature partly counterbalances the biological effect. The temperature generated diurnal pCO_2 maximum occurs approximately at the same time in the afternoon with the production generated the daily pCO_2 minimum. However, this temperature effect is significantly smaller than the production effect.

The largest observed and modeled biological pCO_2 diurnal variability occurs in August, and is twice as large as the one observed one during the spring bloom. On one hand, the temperature is at its annual maximum in July-August, which favors phytoplankton growth, but on the other hand, the solar irradiance is already decreasing from its annual maximum in June-July. During the spring bloom, Chlorophyll A fluorescence was high compared to the one during August, when highest pCO_2 variation is observed. The microbial part of the respiration is highly governed by the temperature, and thus the highest microbial respiration is also expected in the July-August contributing to the large amplitude of the diurnal cycle. It is possible that in

https://doi.org/10.5194/os-2020-115
Preprint. Discussion started: 23 December 2020

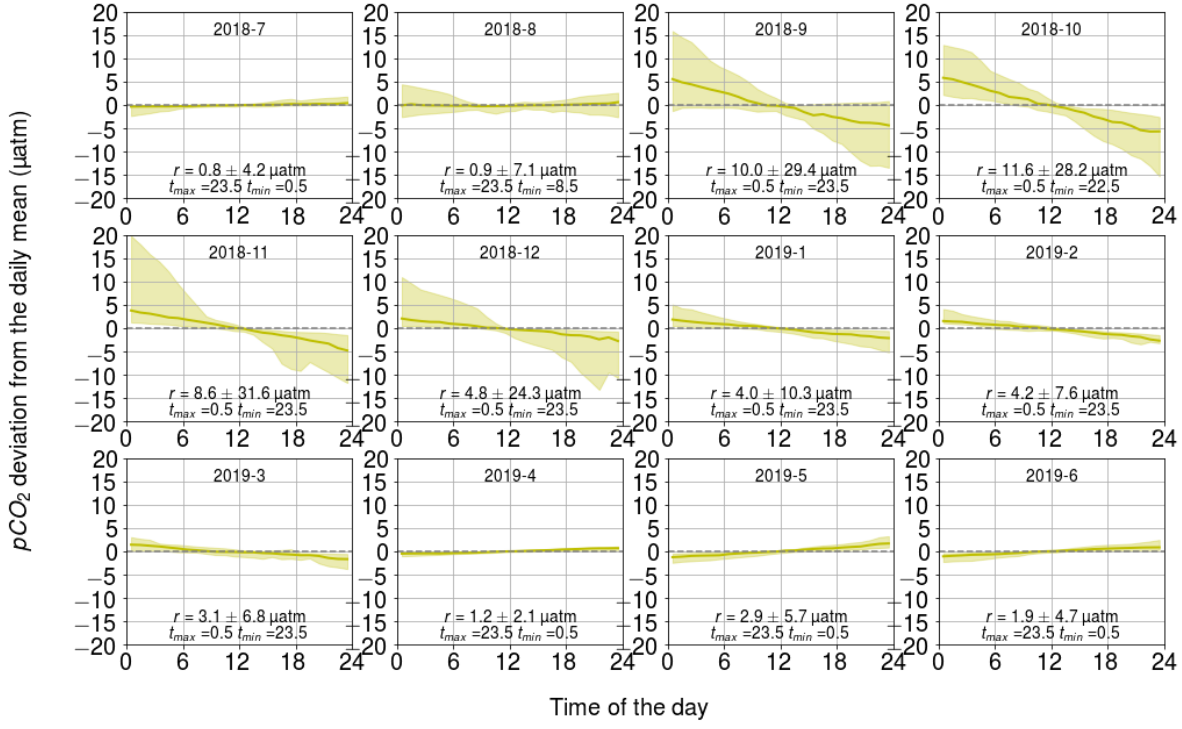

Figure 6. Monthly pCO_2 diurnal variability generated by air-sea exchange of carbon dioxide, showing the binned median and difference of minimum of 10th and maximum of 90th percentiles. The y-axis has the pCO_2 deviation in $\mu\mathrm{atm}$ and the x-axis is the hour of the day. Range, r, and the time for the maximum and minimum pCO_2 are also given.

spring, the daily pCO_2 signal is less pronounced than in autumn due to the deeper mixed layer in spring (Fig. 1a) causing the production to be more diluted than in the case of shallower mixed layer.

Our data set suggests that on average the biological component controls pCO_2 diurnal variability, but on specific days during the biological season, other components can have greater effect as have Wesslander et al. (2011) shown.

During winter, the diurnal pCO_2 pattern generated by the biological processes is an increasing trend, which could indicate mineralisation of organic matter. This kind of trend is, however, not seen in observed pCO_2. This could be due the CO_2 release to the atmosphere counterbalancing the biological effect. This could be the case for the November, but as it is unplausible that the mineralisation would occur effectively for the whole winter.

https://doi.org/10.5194/os-2020-115
Preprint. Discussion started: 23 December 2020

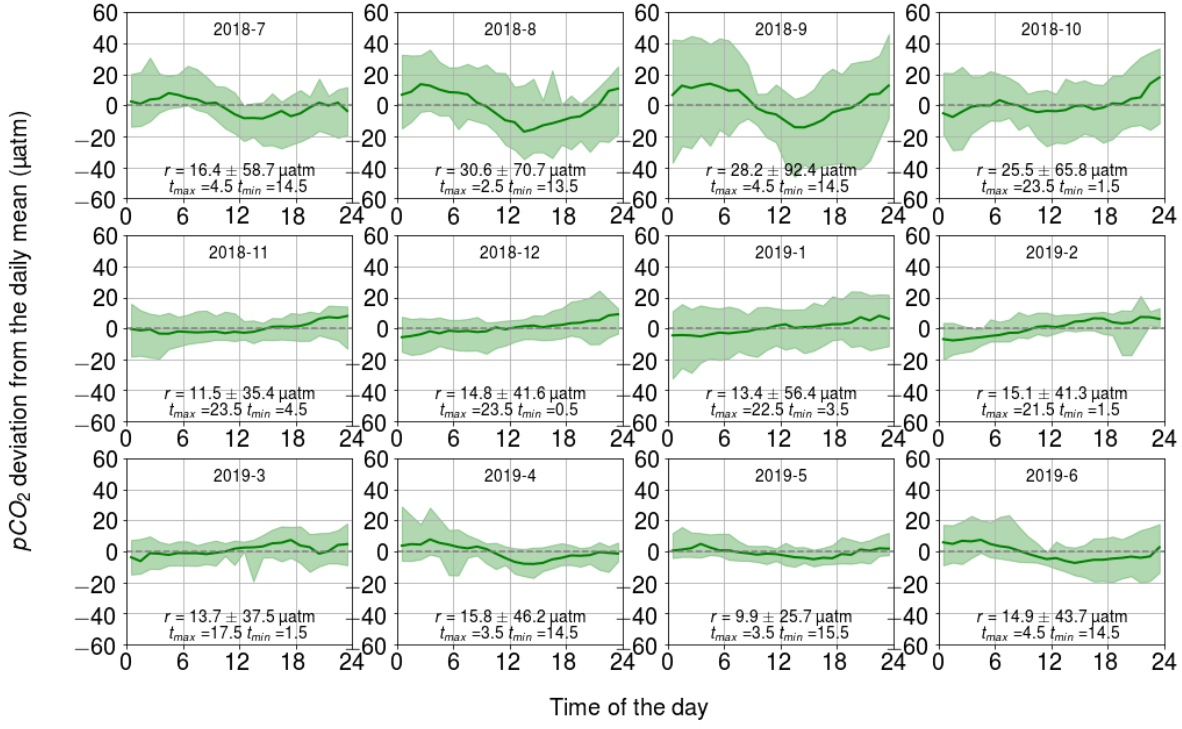

Figure 7. Observed monthly pCO_2 diurnal variability generated by biological transformations, showing the binned median and difference of minimum of 10th and maximum of 90th percentiles. The y-axis has the pCO_2 deviation in $\mu\mathrm{atm}$ and the x-axis is the hour of the day. Range, r, and the time for the maximum and minimum pCO_2 are also given.

4.2.5 Comparing observed and estimated pCO_2 variability

When comparing the observed hourly change in pCO_2 and the calculated change that takes into account all three processes (air-sea exchange, biology and temperature), we found a reasonable correlation. The correlation coefficient was 0.51 ($p < 0.001$), which lends credibility to our approach. The correlation coefficient shows monthly variation (Fig. 8). In April, the highest correlation is found with the value of 0.89 ($p < 0.001$), and the lowest one in July ($R^2 = 0.55$, $p < 0.001$).

The root mean square error ($RMSE$) between all hourly modeled and observed pCO_2 changes was 10 $\mu\mathrm{atm}$. $RMSE$ was 9-14 $\mu\mathrm{atm}$ in July-October, while it was less 3–6 $\mu\mathrm{atm}$ during the other seasons. The scatter in Fig. 8 is visibly highest in July-October. These months showed the highest diurnal pCO_2 variability (see next chapters), which may have a direct effect on the increased error. We divided the monthly $RMSE$ values with the monthly means of the absolute hourly pCO_2 changes to find out this sensitivity variable to be 1.26 on average in March-October, whereas in November-February it was 3.29 on average. Thus, the error introduced by the model during these winter months, though comparatively small in its absolute value,

https://doi.org/10.5194/os-2020-115
Preprint. Discussion started: 23 December 2020

Ocean Science
Discussions
Open Access
EGU

is large compared to the observed variability, which suggests that the estimates of the biological component during the winter time should be treated with cautious. This, however, does not have a significant effect on the analysis, since the biological activity in winter is negligible (see Fig. 1c).

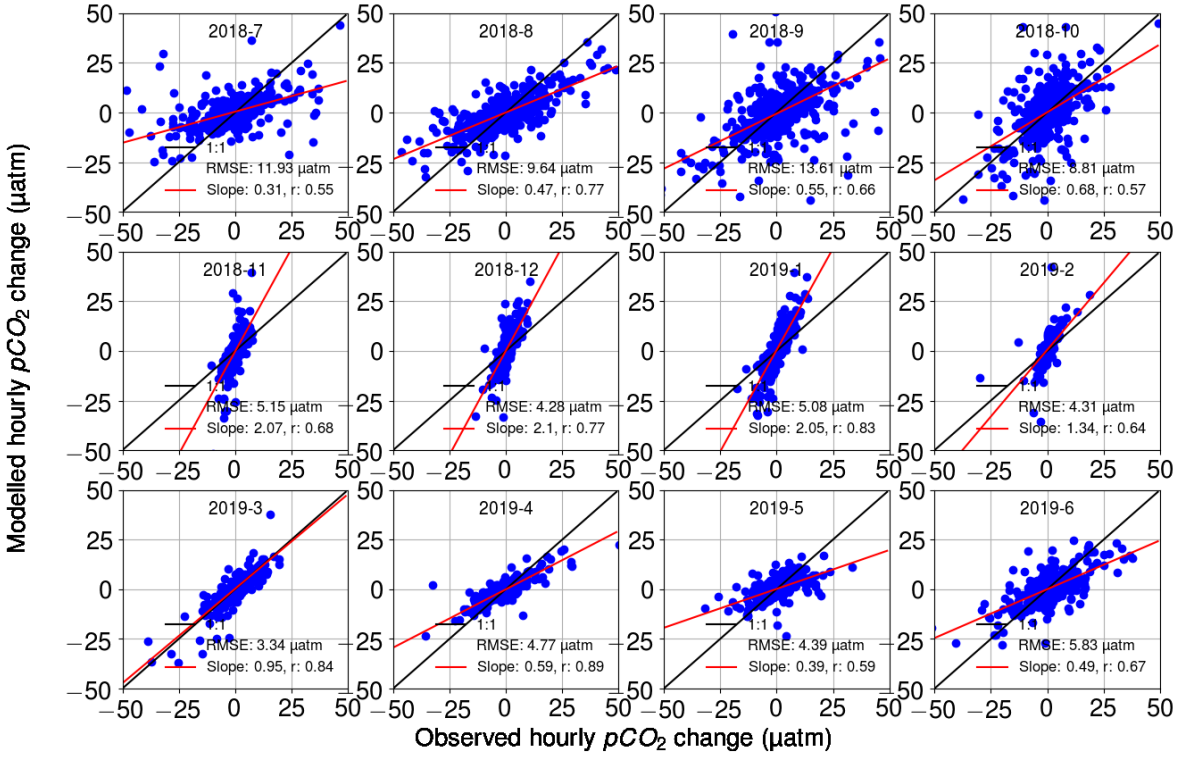

Figure 8. Modelled hourly pCO_2 change (µatm) as a function of observed pCO_2 change (µatm). For each month, the root mean square error between the model and the observation is given, in addition to the slope of the best fit (red line) with its correlation coefficient. Black line is the identity (1:1) line.

The fitted slope between the modeled and observed hourly pCO_2 changes appears to vary during the seasons. During the early winter months (November–January), the modeled pCO_2 changes are twice as large as the observations (slope of 2.1). During the late winter (February-March), the model and observations give the closest match with the slopes of 1.0–1.3. From April to October, the slope varied between 0.3–0.7, with the smallest slopes in July (0.3) and May (0.4). Most of the variation in the modeled pCO_2 orginates from the oxygen-derived biological processes (See next chapters), and thus we argue that the different slopes in observations and modeled data are related to the parameterization of the biological processes. To seek out the possible error sources we produced similar plots as in Fig. 8 but disabling the oxygen flux between the atmosphere and sea

https://doi.org/10.5194/os-2020-115
Preprint. Discussion started: 23 December 2020


Ocean Science
Discussions
Open Access
EGU

and also all other processes (temperature and air-sea CO_2 flux), but these changes proved to have only negligible effect on the slopes. The crude assumption of evenly distributed DIC within the mixed layer does not take into account that large vertical gradients in DIC can be present in the water column. Photosynthesis is most pronounced in the immediate surface promoting the decrease of DIC whereas in the deeper water the mineralisation of organic carbon prevails generating larger DIC. Thus, in some cases this assumption can lead to too high presentations of DIC in the surface.

Possible error sources include the carbon-oxygen ratio in Eq. 4. The Redfield ratio for CO_2-O_2 (-0.77) used in this paper is based on the average oceanic conditions (Redfield et al., 1963). The slopes between the model and the observations (-0.3 – -2.1) suggest that in winter the CO_2-O_2 ratio should be -0.37 and in some summer months as high as -2.5. Due to the lack of photosynthetical radiation in winter the respiration must prevail. Wesslander et al. (2011) determined the CO_2-0_2 ratio in April 2006 in the Baltic Proper to be -1.0 with some diurnal variation. The CO_2-O_2 ratio of respiration (respiratory quotient) depends on the organic substrate in question, the degree of its oxidation and the methabolic pathway used: this quotient may vary between -0.13 and -4.00 (Robinson, 2019): the low (-0.37) winter ratio falls between the ratios of lipids such as $C_{40}H_{74}O_5$ (-0.13) and methane (-0.50). In summer time, photosynthesis takes place. The photosynthetic quotient (here, ratio of carbon dioxide assimilated to oxygen released, CO_2-O_2) could be as high as -2.5 in July, which is very high compared to typical values (Laws, 1991).

4.3 Effects on the air-sea exchange of CO_2

The diurnal pCO_2 variability can have a significant effect on the instantaneous air-sea CO_2 fluxes. The sign of the integrated daily air-sea CO_2 flux can even change, as was observed on the 22nd of July and on 2nd of September (data not shown).

Largest observed monthly median ranges in pCO_2 occurred in July-September (27-31 µatm). During this time the pCO_2 varied from slightly above 100 µatm to 800 µatm. In addition to the surface turbulence, the CO_2 partial pressure difference between the sea and the atmosphere dictates the air-sea flux. The atmospheric CO_2 partial pressure is approximately constant when compared to the to the variability in the surface water. The greatest relative effect on the daily flux occurs when the sea pCO_2 varies close to the atmospheric one, i.e. at approximately 400 µatm. In late July and early August 2018, the sea was a sink and in late August and September, the sea was a source at the study site. The diurnal pCO_2 variability during these months are similar, with a maximum before noon and minimum in the afternoon. Thus, in late July and early August, the pCO_2 difference between the sea and atmosphere is smallest before noon and largest afternoon. In late August and September, the situation is vise versa: largest difference before noon and smallest afternoon.

The discussion above takes into account only the diurnal pCO_2 variation even though the flux also depends on the gas transfer velocity. This might also contain diurnal cyclicity, especially during clear skies on the coastal regions, where spatially uneven heating of the ground generates pressure gradients and thus winds. The most popular parametrisation for gas transfer velocity, i.e. the one by Wanninkhof (1992), is a quadratic function of the wind speed and thus even small changes in wind speed have large impact on the flux.

We calculated how the annual net exchange of carbon dioxide between the sea and atmosphere would vary depending on the sampling time (Fig. 9). The calculations were performed using the flux parametrisation of Wanninkhof (2014). The reference

https://doi.org/10.5194/os-2020-115
Preprint. Discussion started: 23 December 2020

Ocean Science
Discussions
Open Access
EGU

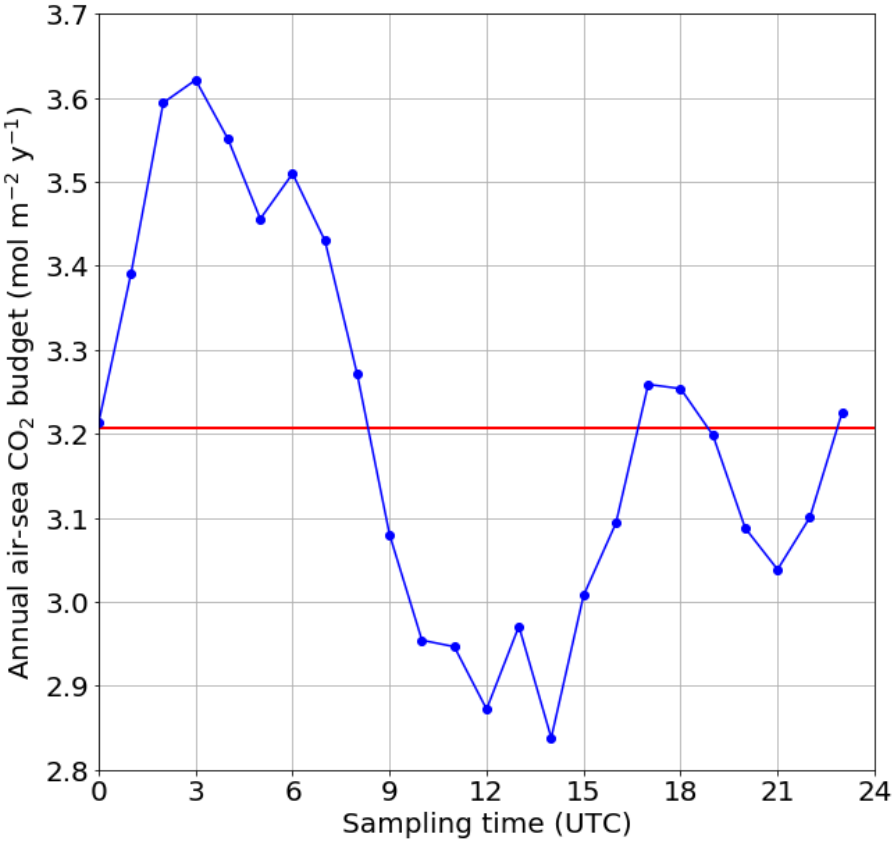

Figure 9. Annual net exchange of carbon dioxide between the sea and atmosphere if only one measurement per day is used. The reference (red line) is based on high frequency data.

net exchange (red line in Fig. 9) is calculated using high frequency one hour data, whereas the other fluxes are calculated using only one measurement per day. The closest match with the high frequency net exchange is captured when sampling the seawater at 9, 17-18 or 24 h UTC. Sampling between 0 and nine o'clock generates an overestimation of the net exchange by up to 12%, whereas sampling between 9 and 18 h leads to an underestimation of up to -12%. The sinusoidal shape of the net exchange as a function of the sampling time clearly originates from the biological component, but the deviation from the sinusoid around 15–20 h must originate from the turbulence parametrisation (wind speed) as such shape is not observed in the pCO_2.

5 Conclusions

The diurnal variability of the CO_2 partial pressure and the contributions of its drivers were studied at Utö station in the Archipelago Sea, the Baltic Sea. At this location, the largest variability was found to take place during July-September, when

https://doi.org/10.5194/os-2020-115
Preprint. Discussion started: 23 December 2020

the monthly median of the diurnal pCO_2 varied in the range of 27-31 µatm. This pCO_2 variability was mostly generated by the biological transformations (production and respiration). However, individual days may show higher variation: pCO_2 varying within 500 µatm a day was attributed to the mixing of water masses.

Assessment of the annual air-sea flux based on the entire data set or individual one hour sampling times, respectively, revealed a potential bias caused by the time of sampling of up to 12%. This finding suggests that data from moving platforms like recearch vessels or voluntary observing ships can have a substantial bias depending on the time of sampling, which might lead to biases in flux calculations or estimation of natural variability.

These findings emphasize the importance of continuous measurements at fixed locations providing temporal coverage on processes, in addition to VOS-lines providing spatial coverage. Autonomous high frequency measurements of carbonate system at fixed sites have proved to be valuable in the assessment of short-term variability of carbonate system (Gac et al., 2020). As European seas are spatially highly heterogeneous, we need organized efforts to map the diurnal variability of the carbon system.

Data availability. TEXT

The data used in this paper can be found in the Zenodo repository (https://doi.org/10.5281/zenodo.4292384).

Appendix A: Air-sea exchange of CO_2

The CO_2 exchange between the atmosphere and the sea, F_{as}, is driven by the difference in CO_2 partial pressure ($\Delta pCO_2 = pCO_2 - pCO_2^{\mathrm{atm}}$) between the surface seawater and atmosphere, or more precisely the differences in fugacity, which refers to the effective partial pressure of CO_2 that takes into account the non-ideal gas behaviour of CO_2. CO_2 partial pressure and fugacity differ only slightly and for this reason, only partial pressure is used from now on. The efficiency of the exchange through the diffusive boundary layers of the gas and liquid fluids is defined by the gas transfer velocity, k. Thus, F_{as} may be written as:

$$F_{as} = kK_0\Delta pCO_2, \tag{A1}$$

where K_0 is the solubility constant of CO_2.

The effect of kinematic viscosity of seawater and the diffusion efficiency of CO_2 on k are taken into account by including the ratio of momentum diffusivity to mass diffusivity, the Schmidt number (Sc), in k:

$$k = k_{660}\left(\frac{Sc}{660}\right)^{-1/2} \tag{A2}$$

Since the Schmidt number is a function of temperature, it is normalized with the Sc of seawater at 20 °C, value of 660. k_{660} is most commonly parameterized by using a wind speed measured at 10 m (U_{10}), and probably the most well known parametrization is a quadratic relationship proposed by Wanninkhof (1992), which was revised by Wanninkhof (2014):

$$k_{660} = 0.251{U_{10}}^2 \tag{A3}$$

https://doi.org/10.5194/os-2020-115
Preprint. Discussion started: 23 December 2020


Ocean Science
Discussions
Open Access
EGU

Appendix B: The inorganic carbon system

Gaseous CO_2 dissolves into water, where part of it hydrates to carbonic acid (H_2CO_3). Dissolved CO_2 and carbonic acid are not easily distinguished, and thus the sum of their concentrations is denoted as $[CO_2^*]$,

$$[CO_2^*] = [CO_2] + [H_2CO_3] \tag{B1}$$

Henry's law describes the relationship between the fugacity of gaseous CO_2, that is in equilibrium with the underlying water, and the dissolved concentration of CO_2,

$$K_0 = [CO_2^*]/pCO_2 \tag{B2}$$

Carbonic acid dissociates to hydrogen carbonate (HCO_3^-, also known as bicarbonate) which further dissociates to carbonate ion (CO_3^{2-}). The equilibrium states:

$$K_1 = \frac{[H^+][HCO_3^-]}{[CO_2^*]} \tag{B3}$$

$$K_2 = \frac{[H^+][CO_3^{2-}]}{[HCO_3^-]} \tag{B4}$$

Solubility constant and the dissociation constants (K_1 and K_2) depend on the free energy of the reaction and thus are functions of temperature and pressure. As these stoichiometric constants are defined using concentrations instead of ion activities, they are also a function of salinity.

Dissolved carbon dioxide, carbonic acid, bicarbonate and carbonate ions form the pool of total dissolved inorganic carbon (DIC):

$$DIC = [CO_2^*] + [HCO_3^-] + [CO_3^{2-}] \tag{B5}$$

DIC is a conservative quantity, i.e. it does not vary as temperature or pressure change. The concentrations of different DIC species change but the sum of these concentrations remains the same if no carbon is added to or removed from the system.

If nutrients and photosynthetically active radiation are available, dissolved CO_2 is transformed into organic matter through the process of photosynthesis. When phytoplankton and other aquatic organisms respirates, the opposite occurs and CO_2 is released. Through microbial degradation in water or in sediments, dissolved organic matter is transformed again into inorganic carbon.

Of all parameters of carbonate system, one can measure only pCO_2, DIC, TA and pH (negative logarithm of hydrogen concentration). To gain the complete description of the carbonate system, one should know at least two of these variables in addition to the information of seawater temperature (T), salinity (S) and pressure (P). Ideally, the effect of dissolved organic matter on total alkalinity should be also known. From Henry's law (Eq. B2), we see that CO_2 fugacity depends on the solubility constant and dissolved CO_2 concentration. Both of these variables are functions of temperature, salinity and pressure. The non-conservativity of $[CO_2^*]$ is due to the effect of dissociation constants, K_1 and K_2.

https://doi.org/10.5194/os-2020-115
Preprint. Discussion started: 23 December 2020


Ocean Science
Discussions
Open Access
EGU

Appendix C: Total alkalinity

Another important variable for the carbonate system is total alkalinity (TA), which is defined as the excess of proton acceptors (acids) over donors (bases). For most practical purposes, it is sufficient to include only carbonate alkalinity, boron alkalinity and a component from the self-dissociation of water, which is commonly referred to as practical alkalinity.

$$\begin{aligned} TA = & \underbrace{[\mathrm{HCO_3^-}] + 2[\mathrm{CO_3^{2-}}]}_{\text{Carbonate alkalinity}} \\ & + \underbrace{[\mathrm{B(OH)_4^-}]}_{\text{Borate alkalinity}} \\ & + \underbrace{[\mathrm{OH^-}] - [\mathrm{H^+}]}_{\text{Self-dissociation of water component}} \\ & \pm \text{minor TA components} \end{aligned} \tag{C1}$$

Minor TA components include organic ions, which may have a large regional impact. In case of the Baltic Sea, the bulk dissolved organic matter has been shown to act as proton acceptor (Kuliński et al., 2014). Similarly to DIC, TA is a conservative quantity.

Calcium carbonate ($\mathrm{CaCO_3}$) is formed in a slow precipitation process by specific calcifying organisms. The precipitation and dissolution of $\mathrm{CaCO_3}$ affect both DIC and TA. However, in the case of the Baltic Sea, there exists calcifying phytoplankton only in the areas next to the North Sea (Tyrrell et al., 2008), and thus, the formation of $\mathrm{CaCO_3}$ can be excluded in calculations for most parts of the pelagic Baltic Sea, including our study site. On the other hand, the weathering of fluvial $\mathrm{CaCO_3}$ has a determinant effect on TA in the limestone-rich southern regions of the Baltic Sea (Müller et al., 2016).

C1 Salinity relationship

For the carbonate system calculations, we used the pair of TA and pCO_2. Whereas pCO_2 was measured, TA was calculated from salinity using an empirical relationship, which was determined based on the direct total alkalinity measurements carried out at Utö in 2017 (Lehto, 2019). The least squares fit of the relationship between the salinity and the directly measured total alkalinity (Fig. C1) had a R^2 value of 0.91.

$$TA = 123.3 + 221.8 \cdot S, \tag{C2}$$

where salinity is unitless and total alkalinity has the unit of $\mu\mathrm{mol\,kg^{-1}}$. The root mean square error between the measurements and the fit is $11.1 \mu\mathrm{mol\,kg^{-1}}$. The slope of this fit is very similar to the parametrisation of $TA - S$ relationship for the Gulf of Bothnia by Müller et al. (2016) extrapolated for year 2017 (220.9 $\mu\mathrm{mol\,kg^{-1}\,PSU^{-1}}$).

https://doi.org/10.5194/os-2020-115
Preprint. Discussion started: 23 December 2020

Ocean Science
Discussions
Open Access
EGU

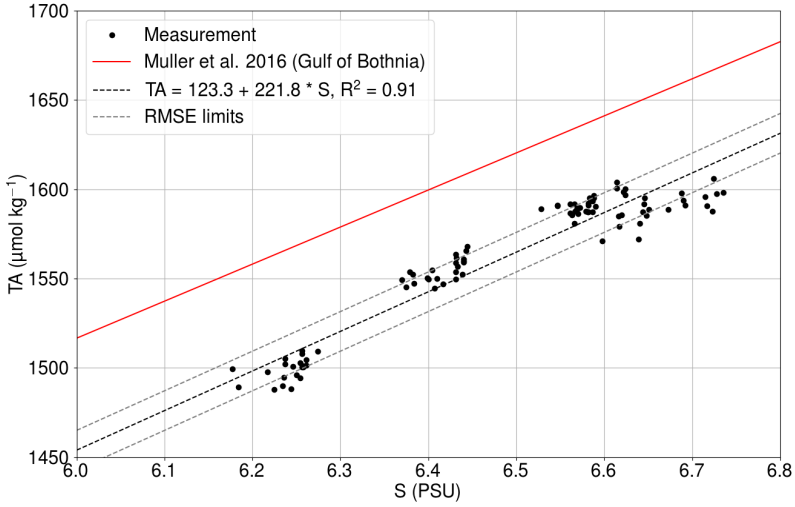

Figure C1. Measured total alkalinity (black dots) as a function of salinity in Utö in 2017 (Lehto, 2019). Solid red line shows the TA-S relationship for Gulf of Bothnia given by Müller et al. (2016). Black dashed line is the best fit, and gray dashed lines show the same line with the limits of root mean square errors.

Appendix D: Gas transfer velocity

We patched the CO_2 air-sea flux time series using a U_{10} based parametrization for k_{660} proposed by Wanninkhof (2014). The applicability of this parametrization for the western marine region of Utö was assessed by calculating k_{660} from the measured CO_2 air-sea flux (from eddy covariance), partial pressure difference, solubility (Weiss, 1974) and Schmidt number (Wanninkhof, 1992). Only cases with southwestern (180–330 °) winds and strong pCO_2 difference (>30 µatm) were considered. CO_2 flux outliers were discarded so that we included only the fluxes that are within the two standard deviations from the median.

Non-stationarity is one of the determinant factors for the quality of direct flux measurement, and thus, non-stationary fluxes are discarded. Here, this means that the mean of 5 min fluxes can deviate less 30% from the 30 min flux. Fully stationary condition is purely theoretical concept, and the threshold for the accepted deviation from this is a matter of choice.

The best quadratic fit ($0.31U_{10}^2$) is only slightly larger than the parametrization proposed by Wanninkhof (2014), and thus we stick with the common parametrization. Low and medium windspeeds are well packed, whereas the 10th and 90th percentiles move further away from each other at high wind speeds. The parametrization of Wanninkhof (2014) shows the highest deviation from the binned median values at highest wind speeds. The binned median at the highest wind speeds is low compared to the Wanninkhof (2014), which may indicate fetch-limitation. More observations at high wind speeds is thus required for the in-depth analysis.

https://doi.org/10.5194/os-2020-115
Preprint. Discussion started: 23 December 2020

Ocean Science
Discussions
Open Access
EGU

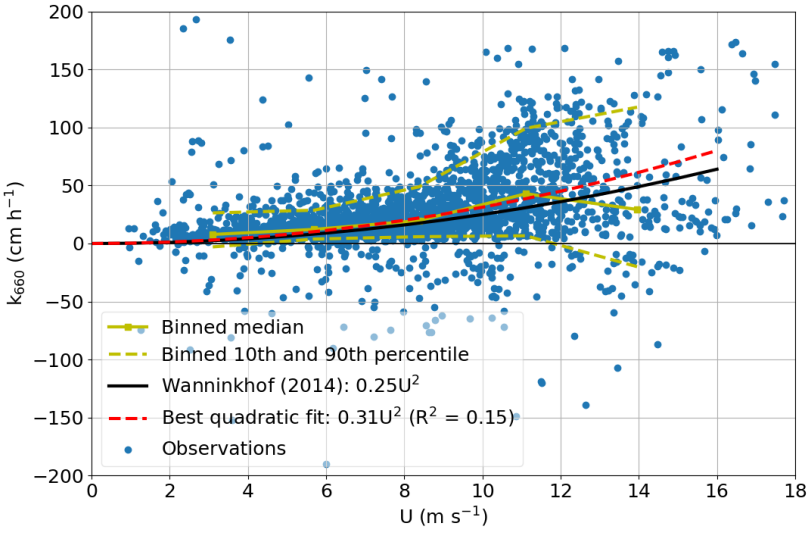

Figure D1. Measured gas transfer velocity as a function of wind speed.

Author contributions. TEXT

MH, LL, JS, JDM and GR were in charge of the conceptualization. MH performed data analysis and visualisation. Manuscript was written by MH, LL, JS, JDM and GR. SK, PY, LL, JS and TM designed and constructed the flow-through system. TM and LL designed and constructed the flux setup. JH is in charge of data management.

Competing interests. TEXT

The authors declare that they have no conflict of interest.

Disclaimer. TEXT

Acknowledgements. Part of this work was supported by the JERICO-NEXT and JERICO-S3 projects, receiving funding from the European Union's Horizon 2020 research and innovation programme under grant agreements no. 654410 and no. 871153, respectively. The BONUS INTEGRAL project funded by the European Union and the Finnish Academy project SEASINK are also acknowledged for the partial funding of this research. The BONUS INTEGRAL project receives funding from BONUS (Art 185), funded jointly by the EU, the German

https://doi.org/10.5194/os-2020-115
Preprint. Discussion started: 23 December 2020

Federal Ministry of Education and Research, the Swedish Research Council Formas, the Academy of Finland, the Polish National Centre for Research and Development, and the Estonian Research Council.

Finnish Marine Research Infrastructure - FINMARI is acknowledged for the funding of the marine research instrumentation. We thank Ismo and Brita Willström for the CTD castings and maintaining the stations, and we thank Anne-Mari Lehto for providing the total alkalinity measurements. Also, thanks are due to the Integrated Carbon Observation System for providing the atmospheric CO_2 data at Utö. We acknowledge Theo Kurten for giving guidance in chemistry and Jani Särkkä for giving guidance in mathematical formulations. CO2SYS program is acknowledged.

https://doi.org/10.5194/os-2020-115
Preprint. Discussion started: 23 December 2020

References

Algesten, G., Brydsten, L., Jonsson, P., Kortelainen, P., Löfgren, S., Rahm, L., Räike, A., Sobek, S., Tranvik, L., Wikner, J. and Jansson, M.: Organic carbon budget for the Gulf of Bothnia, Journal of Marine Systems 63:155–161, https://doi.org/10.1016/j.jmarsys.2006.06.004, 2006.

Andersson, A. J. and Mackenzie, F. T.: Revisiting four scientific debates in ocean acidification research, Biogeosciences, 9, 893–905, https://doi.org/10.5194/bg-9-893-2012, 2012.

Andersson A., Tamminen T., Lehtinen S., Jürgens K., Labrenz M. and Viitasalo M.: The pelagic food web. In: Snoeijs-Leijonmalm P., Schubert H., Radziejewska T. (eds) Biological Oceanography of the Baltic Sea, Springer, Dordrecht, https://doi.org/10.1007/978-94-007-0668-2_8, 2017.

Benson, B. B. and Krause, D.: The concentration and isotopic fractionation of gases dissolved in freshwater in equilibrium with the atmosphere. 1. Oxygen, Limnology and Oceanography, 25, doi:10.4319/lo.1980.25.4.0662, 1980.

Dickson, A. G.: Standard potential of the reaction: AgCl(s) + 12H2(g) = Ag(s) + HCl(aq), and and the standard acidity constant of the ion HSO_4^- in synthetic sea water from 273.15 to 318.15 K, J. Chemical Thermodynamics, 22, 113–127, https://doi.org/10.1016/0021-9614(90)90074-Z, 1990.

Dickson, A. G. and Goyet, C.: Handbook of methttps://doi.org/10.1016/0021-9614(90)90074-Z, hods for the analysis of the various parameters of the carbon dioxide system in sea water, version 2, United States, doi:10.2172/10107773, 1994.

Farcy, P., Durand, D., Charria, G., Painting, S.J., Tamminen, T., Collingridge, K., Grémare, A.J., Delauney, L., and Puillat, I.: Toward a European Coastal Observing Network to Provide Better Answers to Science and to Societal Challenges; The JERICO Research Infrastructure, Front. Mar. Sci. 6:529, doi:10.3389/fmars.2019.00529, 2019.

Feely, R., S. Doney and S. Cooley. Ocean Acidication: Present Conditions and Future Changes in a High-CO_2 World. Oceanography 22(4):36–47. 2009.

Gac J.-P., Marrec P., Cariou T., Guillerm C., Macé É., Vernet M. and Bozec, Y.: Cardinal Buoys: An Opportunity for the Study of Air-Sea CO_2 Fluxes in Coastal Ecosystems, Front. Mar. Sci. 7:712, doi: 10.3389/fmars.2020.00712, 2020.

Garcia, H. E. and Gordon, L. I.: Oxygen solubility in seawater: Better fitting equations, Limnology and Oceanography, 37, https://doi.org/10.4319/lo.1992.37.6.1307, 1992.

Goyet, C. and Peltzer, E. T.: Variation of CO_2 partial pressure in surface seawater in the equatorial Pacific Ocean, Deep Sea Research I, 44(9–10), 1611–1625, 1997.

Honkanen, M., Tuovinen, J.-P., Laurila, T., Mäkelä, T., Hatakka, J., Kielosto, S., and Laakso, L.: Measuring turbulent CO2 fluxes with a closed-path gas analyzer in a marine environment, Atmos. Meas. Tech., 11, 5335-5350, https://doi.org/10.5194/amt-11-5335-2018, 2018.

Kilkki J., Aalto T., Hatakka J., Portin H., Laurila T.: Atmospheric CO2 observations at Finnish urban and rural sites, Boreal Env. Res., 20, 227–242, 2015.

Kraft, K., Seppälä, J., Hällfors, H., Suikkanen, S., Ylöstalo, P., Anglès, S., Kielosto, S., Kuosa, H., Laakso, L., Honkanen, M., Lehtinen, S., Oja, j., Tamminen, T.: Dynamics of bloom-forming filamentous cyanobacteria revealed with high-frequency imaging flow cytometry in the Baltic Sea, Frontiers in Marine Science, Submitted in 2020.

Kuliński, K. and Pempkowiak, J.: The carbon budget of the Baltic Sea, Biogeosciences 8:3219–3230, https://doi.org/10.5194/bg-8-3219-2011, 2011.

https://doi.org/10.5194/os-2020-115
Preprint. Discussion started: 23 December 2020

Kuliński, K., Schneider, B., Hammer, K., Machulik, U. and Schulz-Bull, D.E.: The influence of dissolved organic matter on the acid–base system of the Baltic Sea, Journal of Marine Systems 132, 106–115, https://doi.org/10.1016/j.jmarsys.2014.01.011, 2014.

Kuliński, K., Szymczycha, B., Koziorowska, K., Hammer, K., and Schneider, B.: Anomaly of total boron concentration in the brackish waters of the Baltic Sea and its consequence for the CO_2 system calculations, Marine Chemistry, 204, 11–19, https://doi.org/10.1016/j.marchem.2018.05.007, 2018.

Laakso, L., Mikkonen, S., Drebs, A., Karjalainen, A., Pirinen, P., and Alenius, P.: 100 years of atmospheric and marine observations at the Finnish Utö Island in the Baltic Sea, Ocean Sci., 14, 617-632, https://doi.org/10.5194/os-14-617-2018, 2018.

Lansø, A., Sørensen, L., Christensen, J., Rutgersson, A., Geels, C.: The influence of short-term variability in surface water pCO2 on modelled air–sea CO2 exchange, Tellus B: Chemical and Physical Meteorology, 69, 1302670, 10.1080/16000889.2017.1302670, 2017.

Laws, E.A.: Photosynthetic quotients, new production and net community production in the open ocean, Deep Sea Research Part A. Oceanographic Research Papers, 38(1), 143–167, https://doi.org/10.1016/0198-0149(91)90059-O, 1991.

Lehto, A.-M.: Modelling inorganic carbon system in Utö Baltic Sea, University of Helsinki, MSc Thesis, 2019.

Le Quéré, C., Andrew, R. M., Friedlingstein, P., Sitch, S., Hauck, J., Pongratz, J., Pickers, P. A., Korsbakken, J. I., Peters, G. P., Canadell, J. G., Arneth, A., Arora, V. K., Barbero, L., Bastos, A., Bopp, L., Chevallier, F., Chini, L. P., Ciais, P., Doney, S. C., Gkritzalis, T., Goll, D. S., Harris, I., Haverd, V., Hoffman, F. M., Hoppema, M., Houghton, R. A., Hurtt, G., Ilyina, T., Jain, A. K., Johannessen, T., Jones, C. D., Kato, E., Keeling, R. F., Goldewijk, K. K., Landschützer, P., Lefèvre, N., Lienert, S., Liu, Z., Lombardozzi, D., Metzl, N., Munro, D. R., Nabel, J. E. M. S., Nakaoka, S.-I., Neill, C., Olsen, A., Ono, T., Patra, P., Peregon, A., Peters, W., Peylin, P., Pfeil, B., Pierrot, D., Poulter, B., Rehder, G., Resplandy, L., Robertson, E., Rocher, M., Rödenbeck, C., Schuster, U., Schwinger, J., Séférian, R., Skjelvan, I., Steinhoff, T., Sutton, A., Tans, P. P., Tian, H., Tilbrook, B., Tubiello, F. N., van der Laan-Luijkx, I. T., van der Werf, G. R., Viovy, N., Walker, A. P., Wiltshire, A. J., Wright, R., Zaehle, S. and Zheng, B.: Global Carbon Budget 2018, Earth Syst. Sci. Data, 10, 2141-2194, https://doi.org/10.5194/essd-10-2141-2018, 2018.

Millero, F.J.: Carbonate constants for estuarine waters, Marine and Freshwater Research, v. 61, p. 139-–142, https://doi.org/10.1071/MF09254, 2010.

Müller, J.D., Schneider, B. and Rehder, G.: Long-term alkalinity trends in the Baltic Sea and their implications for CO_2-induced acidification. Limnol. Oceanogr., 61: 1984-200, doi:10.1002/lno.10349, 2016.

Olsen, A., Omar, A. M., Stuart-Menteth, A. C. and Triñanes, J. A.: Diurnal variations of surface ocean pCO_2 and sea-air CO_2 flux evaluated using remotely sensed data. Geophysical Research Letters 31:L20304, doi:10.1029/2004GL020583, 2004.

Orr, J. C., Epitalon, J.-M., and Gattuso, J.-P.: Comparison of ten packages that compute ocean carbonate chemistry, Biogeosciences, 12, 1483–1510, https://doi.org/10.5194/bg-12-1483-2015, 2015.

Redfield, A.C., Ketchum, B.H., and Richards, F.A.: The influence of organisms on the composition of sea-water, The Sea 2:26–77, John Wiley and Sons, New York, 1963.

Robinson, C.J.: Microbial Respiration, the Engine of Ocean Deoxygenation, Frontiers in Marine Science, 5, https://doi.org/10.3389/fmars.2018.00533, 2019.

Saderne, V., Fietzek, P., Herman, P.M.J.: Extreme Variations of pCO_2 and pH in a macrophyte Meadow of the Baltic Sea in summer: Evidence of the effect of photosynthesis and local upwelling. PLoS ONE 8(4):e62689, doi:10.1371/journal.pone.0062689, 2013.

Sarmiento, J.L. and Gruber, N.: Ocean Biogeochemical Dynamics, Princeton University Press, 2004.

Schneider, B., Gülzow, W., Sadkowiak, B. and Rehder, G.: Detecting sinks and sources of CO_2 and CH_4 by ferrybox-based measurements in the Baltic Sea: three case studies. Journal of Marine Systems 140:13–25, http://dx.doi.org/10.1016/j.jmarsys.2014.03.014, 2014.

https://doi.org/10.5194/os-2020-115
Preprint. Discussion started: 23 December 2020

Schneider, B. and Müller, J. D.: Biogeochemical Transformations in the Baltic Sea - Observations Through Carbon Dioxide Glasses, Springer, https://doi.org/10.1007/978-3-319-61699-5, 2018.

Takahashi, T., Olafsson, J., Goddard, J. G., Chipman, D. W. and Sutherland, S. C.: Seasonal variation of CO_2 and nutrients in the high-latitude surface oceans: A comparative study, Global Biogeochemical Cycles 7(4):843—878, https://doi.org/10.1029/93GB02263, 1993.

Tyrrell, T., Schneider, B., Charalampopoulou, A., and Riebesell, U.: Coccolithophores and calcite saturation state in the Baltic and Black Seas, Biogeosciences, 5, 485-494, https://doi.org/10.5194/bg-5-485-2008, 2008.

Wanninkhof, R.: Relationship between wind speed and gas exchange over the ocean, J. Geophys. Res., 97(C5), 7373—7382, https://doi.org/10.1029/92JC00188, 1992.

Wanninkhof, R.: Relationship between wind speed and gas exchange over the ocean revisited, Limnology and Oceanography: Methods 12, doi:10.4319/lom.2014.12.351, 2014.

Wasmund, N., Andrushaitis, A., Lysiak-Pastuszak, E., Muller-Karulis, B., Nausch, G., Neumann, T., Ojaveer, H., Olenina, I., Postel, L., Witek, Z.: Trophic Status of the South-Eastern Baltic Sea: A Comparison of Coastal and Open Areas. Estuarine, Coastal and Shelf Science, 53, 849–864, https://doi.org/10.1006/ecss.2001.0828, 2001.

Weiss, R.F.: Carbon dioxide in water and seawater: the solubility of a non-ideal gas, Marine Chemistry 2(3):203–215, https://doi.org/10.1016/0304-4203(74)90015-2, 1974.

Wesslander, K., Omstedt, A., Schneider, B.: Inter-annual and seasonal variations in the air–sea CO_2 balance in the central Baltic Sea and the Kattegat, Continental Shelf Research 30 1511–1521, https://doi.org/10.1016/j.csr.2010.05.014, 2010.

Wesslander, K., Hall, P., Hjalmarsson, S., Lefevre, D., Omstedt, A., Rutgersson, A., Sahlée, E., Tengberg, A.: Observed carbon dioxide and oxygen dynamics in a Baltic Sea coastal region, Journal of Marine Systems 86. 1–9, https://doi.org/10.1016/j.jmarsys.2011.01.001, 2011.

Yan, H. Yu, K, Shi, Q., Tan, Y., Liu, G., Zhao, M., Li, S., Chen, T. and Wang, Y.: Seasonal variations of seawater pCO_2 and sea-air CO_2 fluxes in a fringing coral reef, northern South China Sea, J. Geophys. Res. Oceans 121:998–1008, doi:10.1002/2015JC011484, 2016.

Ylöstalo, P., Seppälä, J., Kaitala, S., Maunula, P. and Simis, S.: Loadings of dissolved organic matter and nutrients from the Neva River into the Gulf of Finland – Biogeochemical composition and spatial distribution within the salinity gradient, Marine Chemistry, 186:58–71, https://doi.org/10.1016/j.marchem.2016.07.004, 2016.